

Original Research Article

Early results of a remote dosimetry audit program for lung stereotactic body radiation therapy

Burak Yalvac^{*}, Nathalie Reulens, Brigitte Reniers

Universiteit Hasselt, CMK, NuTeC, Diepenbeek, Belgium



ARTICLE INFO

Keywords:

SBRT
 Dosimetry audit
 Alanine/EPR dosimetry
 Radiochromic film dosimetry

ABSTRACT

Background and purpose: A dosimetry audit program based on alanine electron paramagnetic resonance (EPR) and radiochromic film dosimetry, may be a valuable tool for monitoring and improving the quality of lung stereotactic body radiotherapy (SBRT). The aim of this study was to report the initial, independent assessment of the dosimetric accuracy for lung SBRT practice using these dosimeters in combination with a novel phantom design. **Materials and Methods:** The audit service was a remote audit program performed on a commercial lung phantom preloaded with film and alanine detectors. An alanine pellet was placed in the centre of the target simulated using silicone in a 3D-printed mould. Large film detectors were placed coronally through the target and the lung/tissue interface and analysed using gamma analysis. The beam output was always checked on the same day with alanine dosimetry in water. We audited 29 plans from 14 centres up to now. **Results:** For the alanine results 28/29 plans were within 5% with 19/29 plans being within 3%. The passing rates were > 95% for the film through the target for 27/29 plans and 17/29 plans for the film at the lung/tissue interface. For three plans the passing rate was < 90% for the film on top of the lungs. **Conclusions:** The preliminary results were very satisfactory for both detectors. The high passing rates for the film in the interface region indicate good performance of the treatment planning systems. The phantom design was robust and performed well on several treatment systems.

1. Introduction

Stereotactic Body Radiation Therapy (SBRT) is a highly precise and effective radiation treatment technique that delivers high doses of radiation in a few fractions to tumours with minimal damage to surrounding healthy tissues [1–4]. It is rapidly becoming the standard practice for treating lung tumours [5–8]. SBRT is characterised by steep dose gradients outside the treated volume and dose escalation inside the target volume. This requires a very accurate patient setup. The lesions treated with SBRT are often located in difficult heterogeneous regions which causes the dose calculation to be more difficult in these conditions. The treatment planning system (TPS) accuracy must be rigorously verified to ensure safe patient treatment. There is a growing need to ensure the quality and safety of this complex treatment modality. Dosimetry audits are a valuable tool for monitoring and improving the quality of radiotherapy treatments [9]. For SBRT it is recommended that the measurements should be performed in phantoms including low-density lung material and heterogeneous regions to simulate the same physical radiation interactions that occur when treating actual patients.

Several SBRT dosimetry audits and phantom studies have been already reported [10–20].

The choice of the phantom is crucial for a suitable audit program. Anthropomorphic phantoms remain a popular choice. The Imaging and Radiation Oncology Core (IROC) used their custom thorax phantom shell which allowed heterogeneous inserts for lung tissue, tumour and spine material [21]. Motion management was possible on this phantom by placing it on a moving platform. Other auditing networks for SBRT [15,17–19] used different anthropomorphic phantoms allowing heterogeneous inserts for the target and organs at risk (OAR).

We developed an End-to-End (E2E) lung SBRT dosimetry audit program utilising a different anthropomorphic phantom than those mentioned above and using electron paramagnetic resonance (EPR) dosimetry with alanine and radiochromic film dosimetry. This study presents the early results of the lung SBRT dosimetry audit obtained between 2019 and 2022 used to guide the development of the audit protocol. The audit aimed to contribute to the improvement of the overall quality and safety of SBRT practice.

^{*} Corresponding author at: Wetenschapspark 27, 3590 Diepenbeek, Belgium

E-mail addresses: burak.yalvac@uhasselt.be (B. Yalvac), brigitte.reniers@uhasselt.be (B. Reniers).

<https://doi.org/10.1016/j.phro.2024.100544>

Received 31 May 2023; Received in revised form 25 January 2024; Accepted 26 January 2024

Available online 1 February 2024

2405-6316/© 2024 The Author(s). Published by Elsevier B.V. on behalf of European Society of Radiotherapy & Oncology. This is an open access article under the CC BY-NC-ND license (<http://creativecommons.org/licenses/by-nc-nd/4.0/>).

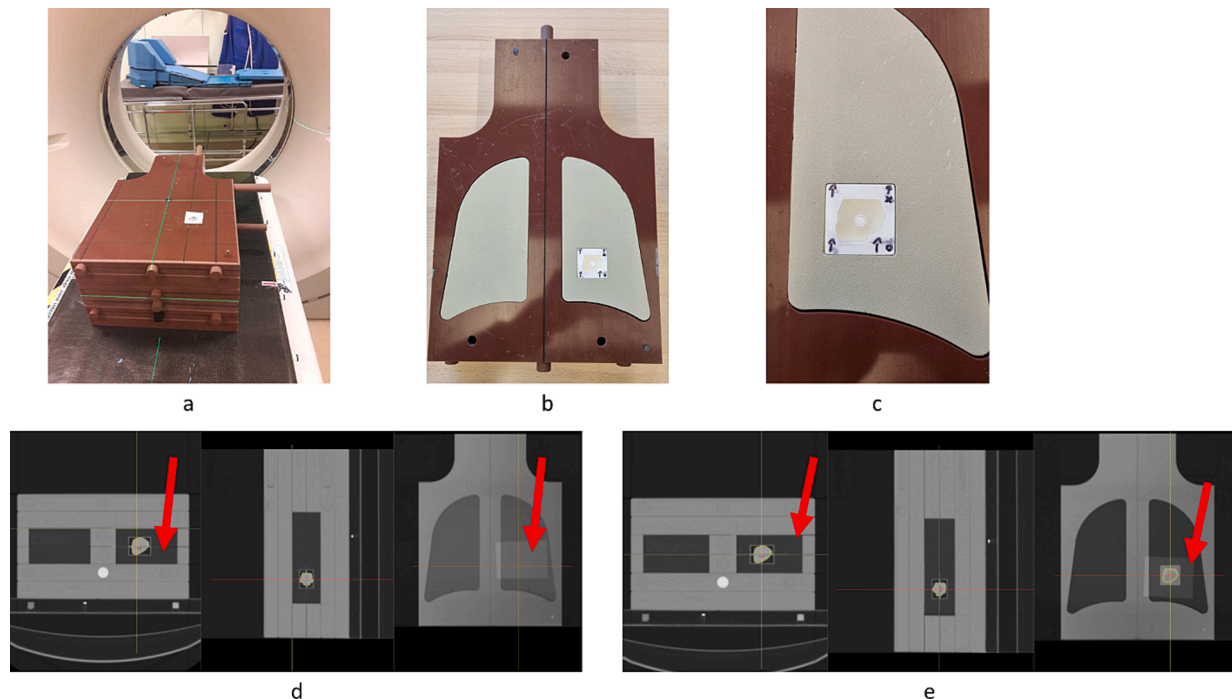


Fig. 1. (a): Positioning of the lung phantom on the gantry. (b): Slab with the lung-equivalent inserts and the 3D-printed mould with tumour and alanine detector (c): Close-up of the tumour and alanine detectors. (d): CT slices of the lung phantom showing the film detector through the target. The red arrows show the film's position (e): CT slices of the lung phantom showing the film detector on top of the lungs. The red arrows show the film's position.

2. Material and methods

2.1. Lung phantom

The IMRT Virtual Water Dose Verification Phantom (Standard Imaging, Inc., Middleton, WI, USA) was used for the audit. The phantom consists of six slabs with 3 cm thickness representing various tissues (e.g. spinal cord, lungs, soft tissue). The phantom includes one bone equivalent plug to simulate the spinal cord. Film detectors could be placed between each slab in the coronal orientation. There were two slabs allowing the placement of lung-equivalent inserts (Fig. 1).

The left lung was modified to include a lung-equivalent 3D-printed polylactic acid (PLA) box which was printed with reduced infill (20 %) to simulate lung tissue. This box served as a mould for a lung tumour ($\pm 9 \text{ cm}^3$) copied from the CT scan of a real patient. This mould was filled with silicone to simulate tumour tissue. An alanine pellet was inserted in the centre of the tumour. The pellet itself was placed in a small 3D-printed cap and this was placed in the silicone. The alanine pellet was used to evaluate the dose to the target. For the evaluation at lower doses and high gradient regions, we relied on film dosimetry benefitting from its superior spatial resolution [22–25]. The film dosimetry was cross-calibrated to the alanine dosimetry, itself calibrated in the Primary Standard Dosimetry Lab (PSDL) of Physikalisch-Technische Bundesanstalt (PTB) [26,27].

Two large pieces ($12 \times 20 \text{ cm}^2$) of Gafchromic EBT-XD films (Ashland Inc., Covington, Kentucky, USA) were placed in the phantom. One film was placed going through the tumour on top of the alanine pellet. The other film was placed on top of the lungs at the interface between the lungs and the soft tissues (Fig. 1).

2.2. SBRT audit methodology

In this remote auditing program performed in Belgium, radiotherapy centres were provided with the audit procedure and materials including the CT scan of the phantom to prepare the audit and the treatment plan. The centres were requested to take a CT scan themselves and prepare the

treatment plan on this scan. The audit procedure contained a questionnaire requesting information about the irradiation unit, the TPS, dose calculation algorithms and grid size. The E2E audit was combined with the basic audit in water including measurements of the output in reference and non-reference conditions. These measurements were performed in a water tank using alanine detectors. This allowed us to obtain basic data about the beam such as beam output and percentage depth doses (PDD) which helped us to understand eventual discrepancies. They were always performed on the same day as the SBRT audit for that particular beam. The centres had to scan the phantom and delineate the structures present in the phantom including the alanine pellet and then prepare an SBRT treatment plan following the local rules of their institution before the audit. The alanine and the films used in this study were calibrated in Dose-to-water ($D_{w,m}$). Consequently, for centres using linear Boltzmann transport equations (LBTE) solver algorithms (Acuros), or Monte Carlo (MC) simulations and reporting in Dose-to-medium in medium ($D_{m,m}$), we asked them to provide a dose distribution in Dose-to-water in medium ($D_{w,m}$) to allow the comparison with our measurements. As the ratio between $D_{w,m}$ and $D_{m,m}$ depends on the atomic compositions of the tissues and the complete geometry of the phantom we chose to let the users perform the conversion in the TPS at the final stage of their dose calculation to remove uncertainties linked to the tissue description. The centres could deliver doses up to 25 Gy to the alanine pellet to not exceed the calibration range of the alanine pellets. Most of the centres delivered one fraction to avoid exceeding the calibration limit but they were allowed to deliver more than one fraction if the total dose remained under 25 Gy.

The centres were also requested to irradiate a polymethyl methacrylate (PMMA) plate set containing film/alanine detectors with the maximum dose in the treatment plan with a uniform field on the same day. This irradiation was used for the “One-scan” [28] rescaling method described in 2.3. After the audit, the centres were requested to ship back the audit material including the filled-in questionnaire and they exported the necessary DICOM data (e.g., CT, RTPLAN, RTSTRUCT, 3D RTDOSE). The centres were also requested to measure the daily output with their local material. This daily output was taken into account for

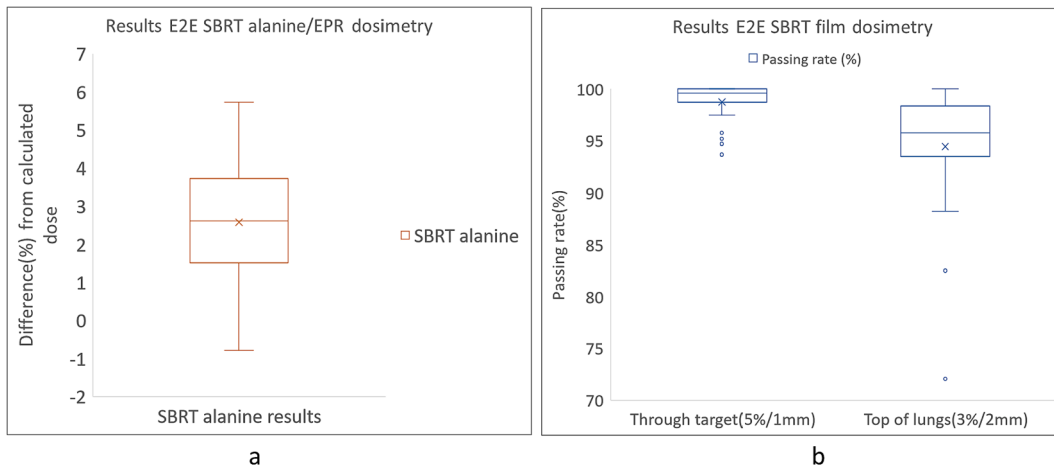


Fig. 2. (a): Summary of the alanine/EPR results for 29 beams (b): Summary of the film dosimetry results for 29 beams for the film through the target using 5%/1mm gamma criteria and for the film on top of the lungs using 3%/2mm gamma criteria.

the comparison with our detectors.

2.3. Dosimetry

To calibrate the film detectors, eight strips of films were irradiated at known doses between 0 and 32 Gy in a geometric progression. The dose delivered to the films was validated using alanine pellets placed in contact with the films at 8 and 16 Gy. The calibration curves were created in FilmQA pro v5.0 and later v7.0 (Ashland Inc., Covington, Kentucky, USA) using a cubic fit. The ‘‘One-scan’’ protocol allowed to compensate for differences in time windows between film irradiation and scanning between the calibration and audit irradiation [28].

The films were scanned on an Epson 10000XL and later an EPSON 12000XL flatbed scanner (EPSON, Suwa, Nagano, Japan) using the Epson driver. The scanner was fitted with the transparency adaptor and scanned in transmission mode. Further details regarding the ‘‘One-Scan’’ protocol and the film read-out can be found in [Supplementary material: Film and alanine dosimetry and audit data](#).

The dose maps were calculated using the triple channel algorithm built in the Film QA Pro software based on Micke et al. [29]. The green channel was used for evaluation because it agreed the best with our alanine/EPR dosimetry. This was verified on 15 prostate IMRT cases by

selecting on the film the region corresponding to the alanine detector in a preliminary unpublished study. The calculated dose maps were projected to the SBRT plans and compared using the gamma evaluation [30,31] method with criteria 5%/1mm global normalization and lower dose threshold (TH) of 10% for the film through the tumour and 3%/2mm global normalization and TH = 10% for the film on top of the lungs. These criteria were chosen based on [32,33].

Cylindrical alanine pellets from Harwell Dosimeters (Oxfordshire, UK) with thickness (h) of 2.8 ± 0.1 mm and diameter of 4.8 ± 0.1 mm were used. The average mass in a batch was ($m = 60 \pm 2$ mg). The alanine pellets consisted of 90.1% of L- α -alanine and 9.9% of paraffin as a binder with 1.2 g/cm^3 as the bulk density. The alanine read-out and analysis were based on [26,27,34–36]. A detailed explanation is given in [Supplementary material: Film and alanine dosimetry and audit data](#).

2.4. Audit data

The results of the E2E SBRT audits between 2019 and 2022 are presented below. Only the results after the follow-up audits were included. The total uncertainty on the alanine read-out was around 1% ($k = 1$) taking into account the uncertainties linked to the intrabatch homogeneity, the EPR amplitude, the temperature during the

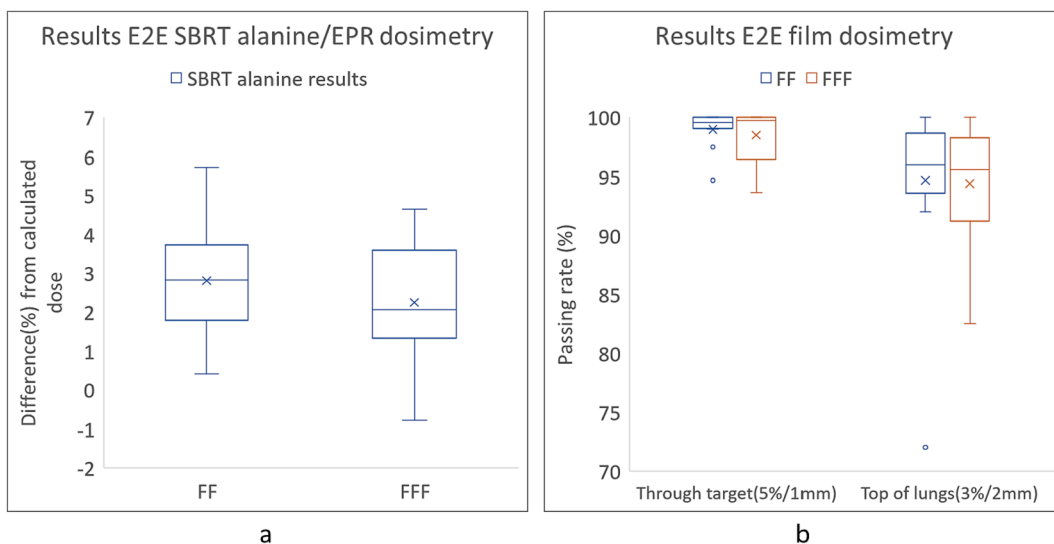


Fig. 3. Summary of the results for FF and FFF beams separately. (a): Summary of the alanine results for 17 FF and 12 FFF beams separately (b): Summary of the film dosimetry results for 17 FF and 12 FFF beams separately.

Table 1

Alanine and film results filtered per algorithm. The number of beams is written in parentheses. The mean deviation between the measured dose by the alanine and the calculated dose is reported per algorithm. The standard deviation is reported in parentheses. For the film results the mean passing rate per algorithm is reported and the standard deviation on the passing rate is reported in parenthesis.

Alanine results		
Algorithm (# beams)	Mean dose difference (%)	Standard deviation (%)
AAA (6)	2.6	2.2
Acuros $D_{w,m}$ (11)	2.3	1.2
CCC (4)	2.1	1.2
Monte Carlo (8)	3.2	0.9
Film results		
Algorithm (# beams)	Mean PR through target 5 %/1mm (st. dev)	Mean PR top of lungs 3 %/2mm (st. dev)
AAA (6)	98.7 (1.8)	94.9 (3.2)
Acuros $D_{w,m}$ (11)	97.6 (2.2)	91.9 (7.7)
CCC (4)	99.9 (0.2)	96.8 (2.6)
Monte Carlo (8)	99.9 (0.2)	97 (2.6)

irradiation, the mass of the pellets, the fading, ... details can be found in [26]. This was documented on the local audit reports. The uncertainty on the film dosimetry based on the consistency maps was around 2 % ($k = 1$) [29,37]. Results were excluded in the case that known human errors had been identified. These were cases of obvious simple errors e.g. wrong positioning of the phantom causing large measured deviation. The audits were performed by the local medical physicists and not by the radiation therapy technologists (RTT). All the results in this paper are corrected by the measured output in reference conditions with the alanine detectors.

The results of 29 audited plans from 14 centres are presented in this study. 17 flattening-filter (FF) beams and 12 flattening-filter-free (FFF) beams were audited. A treatment plan was created for each beam; 28 VMAT plans and one CyberKnife (CK) plan were evaluated. Several algorithms were used, including the Anisotropic analytical algorithm (AAA), collapsed cone convolution (CCC), Acuros $D_{w,m}$ and MC.

A detailed overview is available in Fig. 1 of Supplementary material: Film and alanine dosimetry and audit data.

3. Results

The mean beam output in reference conditions measured with alanine was -1.0% ($\sigma = 0.9\%$). For the alanine results, 28/29 beams were within 5 % with 19/29 beams being within 3 % (Fig. 2a). One beam measured $> 5\%$ variation. The mean dose difference for FF beams was $+2.8\%$ and $+2.2\%$ for FFF beams (Fig. 3a). For the film results, the passing rates were $> 95\%$ for the film through the target for 27/29 beams and 17/29 beams for the film on top of the lungs (Fig. 2b). For three beams the passing rate was $< 90\%$ for the film on top of the lungs. The mean passing rate for FF beams was 98.7 % for the film through the target and 94.7 % for the film on top of the lungs while the mean passing rate for FFF beams was 98.5 % for the film through the target and 94.4 % for the film on top of the lungs (Fig. 3b).

We observed that for 28/29 the measured dose was more than the calculated dose for the alanine/EPR results. The clinical plans in Acuros were usually calculated in $D_{m,m}$ and the recalculation in $D_{w,m}$ introduced on average a 2 % increase of dose in the region of the tumour. When these recalculated plans were compared to the detectors, this difference could not be detected in the passing rates of the films because of the 5 %/1mm constraints but it was detectable with the alanine measurements.

4. Discussion

This paper presents the phantom and the procedure developed in the first phase of the SBRT audits performed between 2019–2022. The alanine results showed satisfactory agreement for most of the cases with 19/29 cases within 3 % of the planned dose. For the films, we chose to emphasise distance to agreement with a 1 mm criterion and 5 % dose difference. This is justified because in SBRT the spatial accuracy is more important due to the hypo-fractionated treatments with high doses per fraction. It was also recommended in the Nederlandse Commissie voor Stralingsdosimetrie (NCS) Report 25 [33]. We added a film on top of the lungs to the audit procedure to give us the possibility in the future to evaluate the performance of the algorithms used in the TPSs in difficult interface regions. As our phantom did not allow motion, there was no validation of the motion management used by the clinics during the treatment of SBRT patients.

Our point dose measurements showed only a slightly higher variation compared to Distefano et al. [6] who also used alanine and film dosimetry in a CIRS thorax phantom. They reported that the dose difference was within $\pm 3\%$ for 25/27 SBRT plans. Dunn et al. [18] reported systematic differences for a pencil beam type algorithm such as AAA in low-density lung region of 2.9 % (Table 1) and we also observed a similar trend (2.6 %).

We have a very good estimate of the uncertainties linked to the alanine detectors provided by PTB. The uncertainty for the films however is closely related to the film scanner and is more difficult to evaluate. A detailed uncertainty budget is still under development. At the moment we chose to use the consistency between the three channels as an estimate.

We observed that our alanine measurements were systematically higher than the calculated doses and this is observed for all algorithms. It is however difficult to draw conclusions about the algorithms themselves with such a limited sample and because the results depend on the configuration of the TPS in each clinic. The conversion between HU and electron density or material should also be specifically checked. For AAA such a trend was expected due to its issues in dose calculation in heterogeneous regions which was also stated in [18]. For the other algorithms, the systematic difference is less expected. One possible reason was the use of silicone as a tumour material which has a higher density (1.32 g/cm^3) and can be incorrectly assigned for cartilage in TPSs. During the development of the audit procedure, it was indeed observed that for this reason, we could not allow the use of $D_{m,m}$ in Acuros as the detectors were calibrated in D_w . Initially, we experimented with gelatine to simulate the tumour as hydrogels are more water equivalent than silicone. This material of the tumour was correctly assigned to soft tissue in the TPS. However, gelatine had short durability which made it impractical for a remote auditing program. The gelatine was consequently replaced by silicone.

We had three audits that required follow-up. All were caused by obvious human errors e.g. wrong positioning of the phantom which caused us to measure an unrealistic huge deviation. The results after follow-up were very good and these are presented in this paper.

The lung phantom used in this study was similar to the popular CIRS thorax phantom used in other studies [15,17–19]. It is also an anthropomorphic phantom containing many heterogeneous regions. One advantage of this phantom and the reason why we chose it was the possibility to place large film detectors through various heterogeneous tissues. The inclusion of the motion is under development.

In the few years of this audit, we noticed a clear transition towards more accurate algorithms such as MC or LBTE-type methods for the majority of the audited centres even if these algorithms require higher computational power for dose calculations. The development of technologies allowing more complex treatment techniques demands the development of more accurate dosimetry. The availability of the phantom proposed here could be used in a specific study to evaluate the dosimetric accuracy of these new algorithms.

In conclusion, the first phase showed promising results. The design of the phantom with the inclusion of the 3D printed box containing a silicone tumour and the use of a combination of alanine dosimeters and films gave very satisfactory results. Improvement concerning among other things such as the material of the tumour is under way.

CRedit authorship contribution statement

Burak Yalvac: Investigation, Resources. **Nathalie Reulens:** Conceptualization, Methodology, Writing – review & editing, Supervision, Project administration, Funding acquisition. **Brigitte Reniers:** .

Declaration of competing interest

The authors declare that they have no known competing financial interests or personal relationships that could have appeared to influence the work reported in this paper.

Acknowledgements

The BELdART project is sponsored by the Cancer Plan and was monitored by the Belgian College of Radiation Oncology between 2009-2022.

Appendix A. Supplementary data

Supplementary data to this article can be found online at <https://doi.org/10.1016/j.phro.2024.100544>.

References

- Andratschke N, Alheid H, Allgauer M, Becker G, Blanck O, Boda-Heggemann J, et al. The SBRT database initiative of the German Society for Radiation Oncology (DEGRO): patterns of care and outcome analysis of stereotactic body radiotherapy (SBRT) for liver oligometastases in 474 patients with 623 metastases. *BMC Cancer* 2018;18:283. <https://doi.org/10.1186/s12885-018-4191-2>.
- Guckenberger M, Andratschke N, Dieckmann K, Hoogeman MS, Hoyer M, Hurkmans C, et al. ESTRO ACROP consensus guideline on implementation and practice of stereotactic body radiotherapy for peripherally located early stage non-small cell lung cancer. *Radiother Oncol* 2017;124:11–7. <https://doi.org/10.1016/j.radonc.2017.05.012>.
- Sahgal A, Roberge D, Schellenberg D, Purdie TG, Swaminath A, Pantarotto J, et al. The Canadian Association of Radiation Oncology scope of practice guidelines for lung, liver and spine stereotactic body radiotherapy. *Clin Oncol (R Coll Radiol)* 2012;24:629–39. <https://doi.org/10.1016/j.clon.2012.04.006>.
- Weber DC, Tomsej M, Melidis C, Hurkmans CW. QA makes a clinical trial stronger: evidence-based medicine in radiation therapy. *Radiother Oncol* 2012;105:4–8. <https://doi.org/10.1016/j.radonc.2012.08.008>.
- Claridge Mackonis ER, Hardcastle N, Haworth A. Stereotactic ablative body radiation therapy (SABR) in NSW. *Phys Eng Sci Med* 2020;43:641–50. <https://doi.org/10.1007/s13246-020-00866-3>.
- Distefano G, Baker A, Scott AJ, Webster GJ and Group USCQA. Survey of stereotactic ablative body radiotherapy in the UK by the QA group on behalf of the UK SABR Consortium. *Br J Radiol* 2014;87(20130681). <https://doi.org/10.1259/bjr.20130681>.
- Pan H, Simpson DR, Mell LK, Mundt AJ, Lawson JD. A survey of stereotactic body radiotherapy use in the United States. *Cancer* 2011;117:4566–72. <https://doi.org/10.1002/cncr.26067>.
- Nagata Y, Hiraoka M, Mizowaki T, Narita Y, Matsuo Y, Narihisa Y, et al. Survey of stereotactic body radiation therapy in Japan by the Japan 3-D Conformal External Beam Radiotherapy Group. *Int J Radiat Oncol Biol Phys* 2009;75:343–7. <https://doi.org/10.1016/j.ijrobp.2009.02.087>.
- Clark CH, Jornet N, Muren LP. The role of dosimetry audit in achieving high quality radiotherapy. *Phys Imaging Radiat Oncol* 2018;5:85–7. <https://doi.org/10.1016/j.phro.2018.03.009>.
- Shaw M, Lye J, Alves A, Lehmann J, Sanagou M, Geso M, et al. Measuring dose in lung identifies peripheral tumour dose inaccuracy in SBRT audit. *Phys Med* 2023;112:102632. <https://doi.org/10.1016/j.ejmp.2023.102632>.
- Greer MD, Koger B, Glenn M, Kang J, Rengan R, Zeng J, et al. Predicted Inferior Outcomes for Lung SBRT With Treatment Planning Systems That Fail Independent Phantom-Based Audits. *Int J Radiat Oncol Biol Phys* 2023;115:1301–8. <https://doi.org/10.1016/j.ijrobp.2022.12.003>.
- Edward SS, M CG, Peterson CB, Balter PA, Pollard-Larkin JM, Howell RM, et al. Dose calculation errors as a component of failing IROC lung and spine phantom irradiations. *Med Phys* 2020;47:4502-8. <https://doi.org/10.1002/mp.14258>.
- Edward SS, Alvarez PE, Taylor PA, Molineu HA, Peterson CB, Followill DS, et al. Differences in the Patterns of Failure Between IROC Lung and Spine Phantom Irradiations. *Pract Radiat Oncol* 2020;10:372–81. <https://doi.org/10.1016/j.prro.2020.04.004>.
- Tsang Y, Carver A, Groom N, Harris C, Favier-Finn C, Eaton D. A multi-centre dosimetry audit on advanced radiotherapy in lung as part of the Isotoxic IMRT study. *Phys Imaging Radiat Oncol* 2017;4:17–21. <https://doi.org/10.1016/j.phro.2017.11.001>.
- Distefano G, Lee J, Jafari S, Gouldstone C, Baker C, Mayles H, et al. A national dosimetry audit for stereotactic ablative radiotherapy in lung. *Radiother Oncol* 2017;122:406–10. <https://doi.org/10.1016/j.radonc.2016.12.016>.
- Clark CH, Hurkmans CW, Kry SF and Global Quality Assurance of Radiation Therapy Clinical Trials Harmonisation G. The role of dosimetry audit in lung SBRT multi-centre clinical trials. *Phys Med* 2017;44:171–6. <https://doi.org/10.1016/j.ejmp.2017.04.003>.
- Lambrech M, Melidis C, Sonke JJ, Adebahr S, Boellaard R, Verheij M, et al. Lungtech, a phase II EORTC trial of SBRT for centrally located lung tumours - a clinical physics perspective. *Radiat Oncol* 2016;11:7. <https://doi.org/10.1186/s13014-015-0567-5>.
- Dunn L, Lehmann J, Lye J, Kenny J, Kron T, Alves A, et al. National dosimetric audit network finds discrepancies in AAA lung inhomogeneity corrections. *Phys Med* 2015;31:435–41. <https://doi.org/10.1016/j.ejmp.2015.04.002>.
- Lambrech ML, Eaton DJ, Sonke JJ, Nestle U, Peulen H, Weber DC, et al. Results of a multicentre dosimetry audit using a respiratory phantom within the EORTC LungTech trial. *Radiother Oncol* 2019;138:106–13. <https://doi.org/10.1016/j.radonc.2019.06.008>.
- Hansen CR, Sykes JR, Barber J, West K, Bromley R, Szymura K, et al. Multicentre knowledge sharing and planning/dose audit on flattening filter free beams for SBRT lung. *J Phys Conf Ser* 2015;573:012018. <https://doi.org/10.1088/1742-6596/573/1/012018>.
- Followill DS, Evans DR, Cherry C, Molineu A, Fisher G, Hanson WF, et al. Design, development, and implementation of the radiological physics center's pelvis and thorax anthropomorphic quality assurance phantoms. *Med Phys* 2007;34:2070–6. <https://doi.org/10.1118/1.2737158>.
- Devic S, Tomic N, Lewis D. Reference radiochromic film dosimetry: Review of technical aspects. *Phys Med* 2016;32:541–56. <https://doi.org/10.1016/j.ejmp.2016.02.008>.
- Gonzalez-Lopez A, Vera-Sanchez JA, Lago-Martin JD. Small fields measurements with radiochromic films. *J Med Phys* 2015;40:61–7. <https://doi.org/10.4103/0971-6203.158667>.
- Palmer AL, Nisbet A, Bradley D. Verification of high dose rate brachytherapy dose distributions with EBT3 Gafchromic film quality control techniques. *Phys Med Biol* 2013;58:497–511. <https://doi.org/10.1088/0031-9155/58/3/497>.
- Menegotti L, Delana A, Martignano A. Radiochromic film dosimetry with flatbed scanners: a fast and accurate method for dose calibration and uniformity correction with single film exposure. *Med Phys* 2008;35:3078–85. <https://doi.org/10.1118/1.2936334>.
- Anton M. Uncertainties in alanine/ESR dosimetry at the Physikalisches-Technische Bundesanstalt. *Phys Med Biol* 2006;51:5419–40. <https://doi.org/10.1088/0031-9155/51/21/003>.
- Anton M. Development of a secondary standard for the absorbed dose to water based on the alanine EPR dosimetry system. *Appl Radiat Isot* 2005;62:779–95. <https://doi.org/10.1016/j.apradiso.2004.10.009>.
- Lewis D, Micke A, Yu X, Chan MF. An efficient protocol for radiochromic film dosimetry combining calibration and measurement in a single scan. *Med Phys* 2012;39:6339–50. <https://doi.org/10.1118/1.4754797>.
- Micke A, Lewis DF, Yu X. Multichannel film dosimetry with nonuniformity correction. *Med Phys* 2011;38:2523–34. <https://doi.org/10.1118/1.3576105>.
- Low DA, Dempsey JF. Evaluation of the gamma dose distribution comparison method. *Med Phys* 2003;30:2455–64. <https://doi.org/10.1118/1.1598711>.
- Low DA, Harms WB, Mutic S, Purdy JA. A technique for the quantitative evaluation of dose distributions. *Med Phys* 1998;25:656–61. <https://doi.org/10.1118/1.598248>.
- Miften M, Olch A, Mihailidis D, Moran J, Pawlicki T, Molineu A, et al. Tolerance limits and methodologies for IMRT measurement-based verification QA: Recommendations of AAPM Task Group No. 218. *Med Phys* 2018;45:e53–83. <https://doi.org/10.1002/mp.12810>.
- Heukelom S, Hermans J, Hoffmans-Holtzer N, Marijnissen H, Nulens A, Pittomvils G, et al. Process Management and Quality Assurance of Intracranial Stereotactic Treatment. Netherlands Commission on Radiation Dosimetry (NCS) 2015;Report 25;0-141.
- Anton M, Kapsch RP, Krauss A, von Voigts-Rhetz P, Zink K, McEwen M. Difference in the relative response of the alanine dosimeter to megavoltage x-ray and electron beams. *Phys Med Biol* 2013;58:3259–82. <https://doi.org/10.1088/0031-9155/58/10/3259>.
- Schaeken B, Cuypers R, Lelie S, Schroyers W, Schreurs S, Janssens H, et al. Implementation of alanine/EPR as transfer dosimetry system in a radiotherapy audit programme in Belgium. *Radiother Oncol* 2011;99:94–6. <https://doi.org/10.1016/j.radonc.2011.01.026>.
- Schaeken B, Cuypers R, Goossens J, Van den Weyngaert D, Verellen D. Experimental determination of the energy response of alanine pellets in the high dose rate 192Ir spectrum. *Phys Med Biol* 2011;56:6625–34. <https://doi.org/10.1088/0031-9155/56/20/007>.
- Vera-Sanchez JA, Ruiz-Morales C, Gonzalez-Lopez A. Monte Carlo uncertainty analysis of dose estimates in radiochromic film dosimetry with single-channel and multichannel algorithms. *Phys Med* 2018;47:23–33. <https://doi.org/10.1016/j.ejmp.2018.02.006>.